Electronic Supporting Information

A Unique and Discrete Ce(III) Macrocyclic Complex Exhibits Ferroelectricity, Dielectric and Slow relaxation of Magnetization

Mohd Wasim, [a] Kamal Uddin Ansari, [a] Pardeep Kumar,[a] Binit Mallick[b] and Maheswaran Shanmugam,*[a]

[a]Department of Chemistry, Indian Institute of Technology Bombay, Powai, Mumbai-400076, Maharashtra, India.

[b]Department of Electrical Engineering, Indian Institute of Technology Bombay, Powai, Mumbai-400076, Maharashtra, India.

Materials and Methods

Selenium dioxide (SeO_2) and o-phenylenediamine (PD) were purchased from Sigma Aldrich and PD was sublimed before use. $Ce(NO_3)_3.6H_2O$ was purchased from Alfa Aesar and used without any further purification. Complex **1** was synthesized using the method reported.[1] The polycrystalline thin film of complex **1** on Si wafer (1 cm x 1 cm) substrate was made by drop-casting the saturated solution of **1** in DMF on Si substrate and evaporation of the solvent under fume hood at ambient condition. The powder X-ray pattern of the bulk sample was recorded through an X-Ray Powder Diffraction instrument (PANalytical, Netherlands). Differential scanning calorimetry (DSC) measurement of **1** was performed on a Pyris 6 DSC (Perkin Elmer). Polarisation vs. electric field (PE) loop, dielectric constant vs. temperature at different fields, and frequency were recorded using Broadband Dielectric Spectrometer (BDS) Concept 80 (Novocontrol Technologies, Germany). Ferroelectric response in thin-film was analyzed using MFP-3D Origin (Asylum/Oxford Instruments) in contact mode with Ti/Ir (5 nm/20 nm) coated AFM tip. Magnetic susceptibility measurements of polycrystalline sample of **1** in the temperature range 1.8–300 K were performed using MPMS-XL SQUID magnetometer (Quantum Design, USA) instrument equipped with 70 kOe superconducting magnet. The second harmonic spectra of pellet sample of **1** was captured using a home build optical setup similar to a widefield microscope except for the detection part. At the detection end, we have used a spectrograph and an EMCCD (Electron Multiplying Charge Coupled Device). The incident 800 nm photon pulse (pulse width 100 fs) is produced using a Ti:Sapphire ultrafast laser (Mai Tai HP from Spectra Physics). The repetition rate of the produced pulse is 80 MHz. Using a neutral density filter and special filter, we have reduced the average power up to 40 mW on the sample. The 800 nm beam first reflected at an angle of 45^0 using a dichroic mirror (Thorlabs Part Number: DMSP567R) and focused onto the sample using a long working distance objective lens (Mitutoyo M Plan Apo SL 20X; N.A.=0.42;

WD=20 mm) at a normal incidence angle. The same lens is used to collect the second harmonic (400 nm) response from the sample. The harmonic response is focused into the inlet of the spectrograph (Shamrock 303i-A from Andor) using a tube lens (Thorlabs Part Number: TTL200) pass through the dichroic and guided to the spectrograph (Shamrock 303i-A from Andor) inlet. The spectra are measured using an EMCCD (Newton EMCCD: DU970P from Andor) connected at the outlet of the spectrograph.

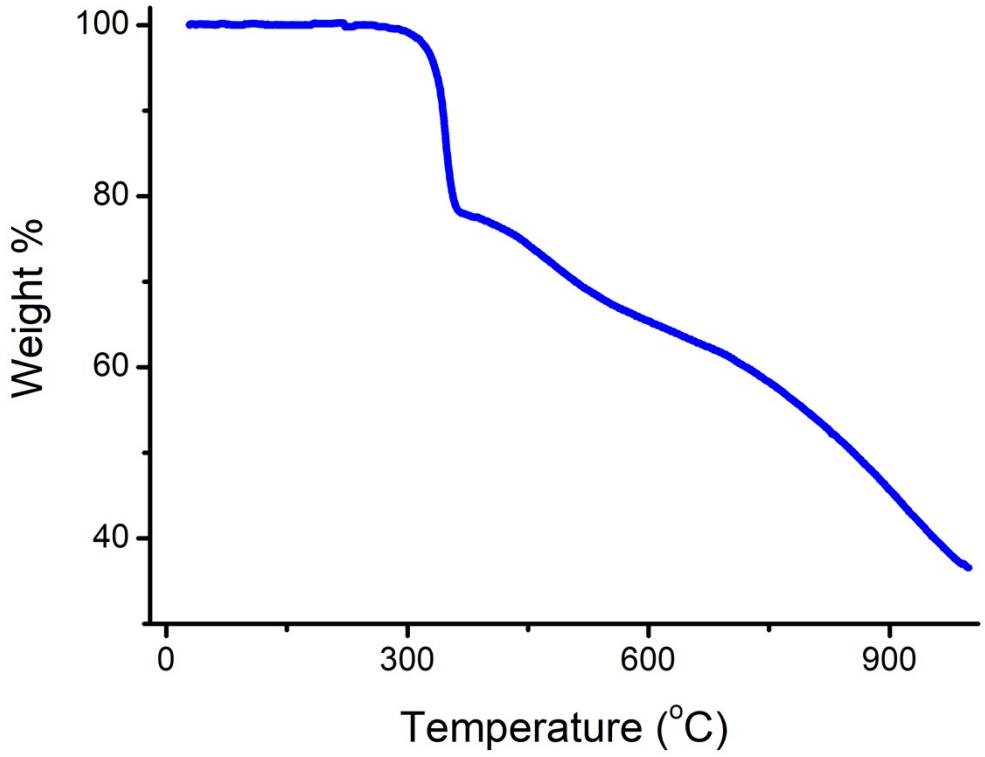

Fig. S1 Thermo gravimetric analysis (TGA) of complex **1**

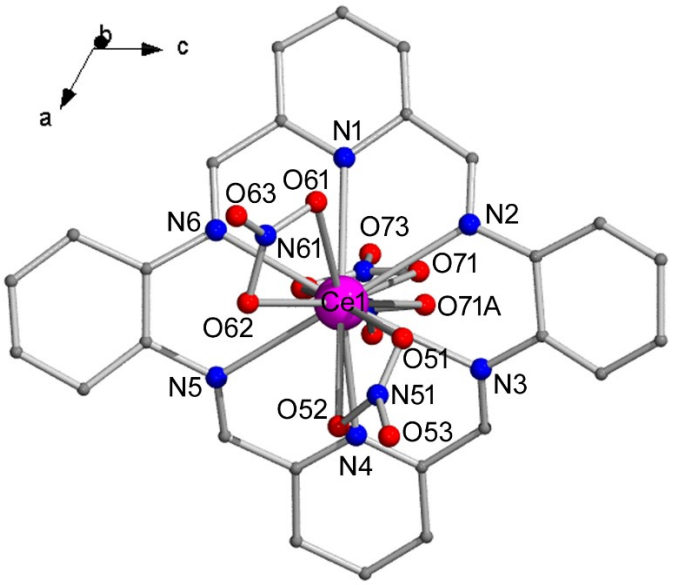

Fig. S2 Ball and stick representation of the molecular structures of complex **1** (planar view along the b-axis). Hydrogen atoms were removed for clarity.

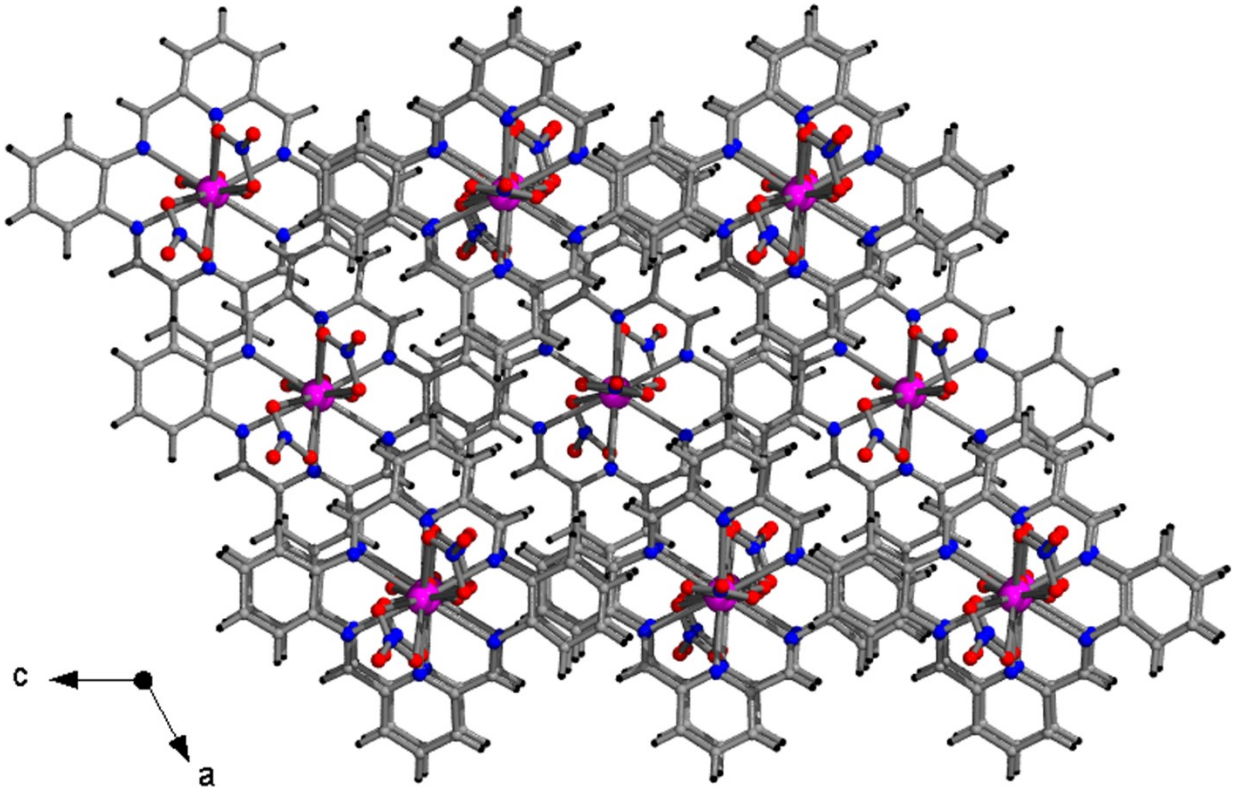

Fig. S3 Packing of complex **1** in ac plane showing π-π stacking and H-bonding. Disordered part of the nitrate was removed for the sake of clarity.

Table S1. Crystallographic parameters for complexes

	1
Formula	$C_{26}H_{18}N_9O_9Ce$
Size (mm)	0.195 × 0.086 × 0.063
System	Monoclinic
Space group	Cc
a [Å]	15.0419(9)
b [Å]	10.8382(5)
c [Å]	19.5595(11)
β [°]	118.139(7)
V [Å^3]	2811.9(3)
Z	4
ρ_{calcd} [g/cm^3]	1.749
$2\Theta_{max}$	50
Radiation	MoK_α
λ [Å]	0.71073
T [K]	298(2)
Reflns	8927
Ind. Reflns	4453
Reflns with >2σ(I)	3607
R_1	0.0596
wR_2	0.1272

Table S2. Selected bond angle and bond distances for **1**

Bond length (Å)		**Bond angle (°)**	
Label	**1**	Label	**1**
Ce1-O51	2.6933(1)	N1-Ce1-N2	60.194(2)
Ce1-O52	2.7587(2)	N2-Ce1-N3	57.211(2)
Ce1-O61	2.6837(2)	N3-Ce1-N4	60.869(2)
Ce1-O62	2.6143(1)	N4-Ce1-N5	61.236(2)
Ce1-O71	2.6715(1)	N5-Ce1-N6	59.165(2)
Ce1-O71A	2.7606(1)	N6-Ce1-N1	59.528(2)
Ce1-O72	2.6100(1)	N1-Ce1-N4	139.427(4)
Ce1-O72A	2.6444(1)	O51-Ce1-O52	45.339(1)
Ce1-N1	2.7046(2)	O61-Ce1-O62	49.197(1)
Ce1-N2	2.7346(2)	O71-Ce1-O72	48.231(1)
Ce1-N3	2.7972(2)	O71A-Ce1-O72A	47.077(1)
Ce1-N4	2.6750(2)	O51-Ce1-O61	66.689(2)
Ce1-N5	2.7482(2)	O52-Ce1-O62	62.703(2)
Ce1-N6	2.6734(2)	O51-Ce1-O71	124.175(1)
		O51-Ce1-O72	168.172(1)
		O52-Ce1-O72	129.802(1)
		O52-Ce1-O71	131.818(1)
		O62-Ce1-O71	165.327(1)
		O62-Ce1-O72	123.418(1)
		O61-Ce1-O71	122.049(1)
		O61-Ce1-O72	124.396(1)

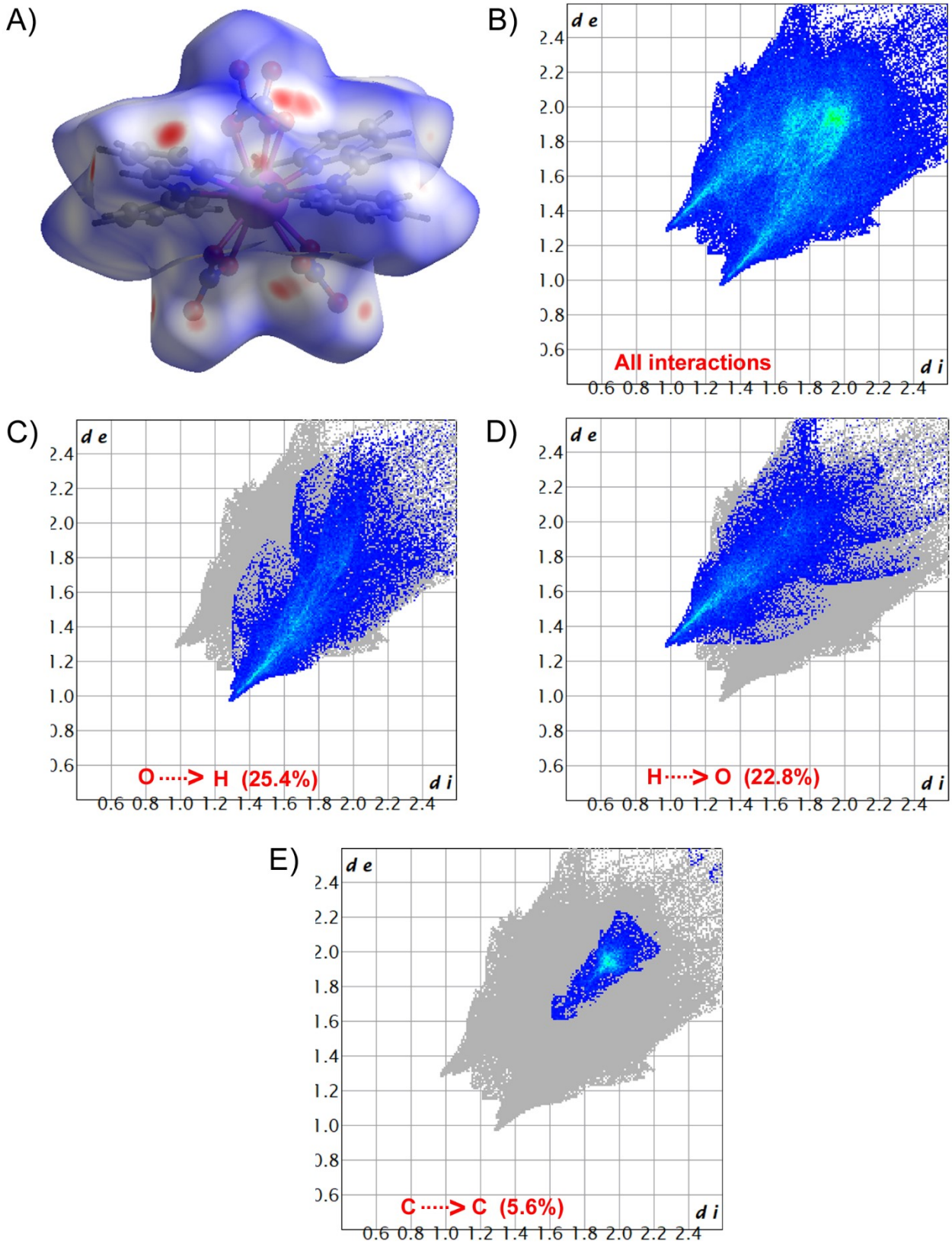

Fig. S4 (A) Hirshfeld surface of **1** mapped with dnorm. (B), (C), (D) and (E) fingerprint plot for non-covalent interactions involving all, inside O – outside H, inside H – outside O, inside C – outside C surfaces respectively. The analysis was done using CrystalExplorer software.[2]

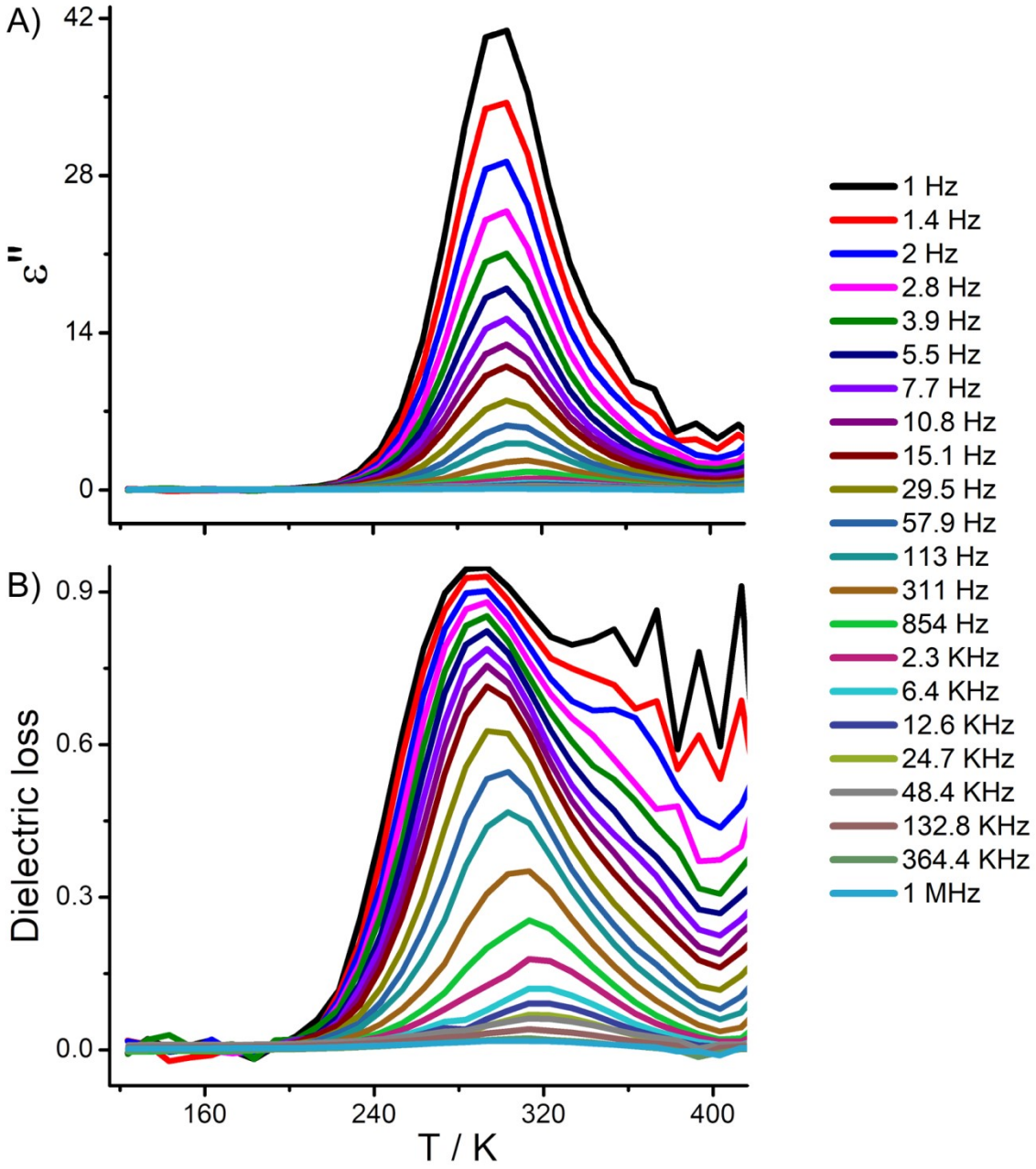

Fig. S5 (A) Temperature dependence of imaginary part of complex dielectric constant and (B) Temperature dependence of dielectric loss in pellet sample of **1**

Table S3 Estimated Curie-Weiss constant for para and ferroelectric phases of **1**

Frequency	C_{para}	C_{ferro}	C_{para}/C_{ferro}
1 Hz	793.65	487.80	1.63
1.4 Hz	751.88	471.70	1.59
2 Hz	724.64	478.47	1.51
2.8 Hz	704.23	497.51	1.42
3.9 Hz	694.44	510.20	1.36
5.5 Hz	689.66	497.51	1.39
7.7 Hz	684.93	510.20	1.34
10.8 Hz	689.66	529.10	1.30
15.1 Hz	699.30	549.45	1.27
25.5 Hz	680.27	649.35	1.05
57.9 Hz	735.29	729.93	1.01
113 Hz	813.01	847.46	0.96
311 Hz	1000	1136.36	0.88
854 Hz	1298.70	1562.50	0.83
2.3 KHz	1754.39	2272.73	0.77
6.4 KHz	2564.10	2941.18	0.87
12.6 KHz	2941.18	3333.33	0.88
24.7 KHz	3571.43	4000.00	0.89
48.4 KHz	4000.00	4761.90	0.84
132.8 KHz	4761.90	5882.35	0.81
364.4 KHz	6250.00	7142.86	0.87
1MHz	7142.86	8333.33	0.86

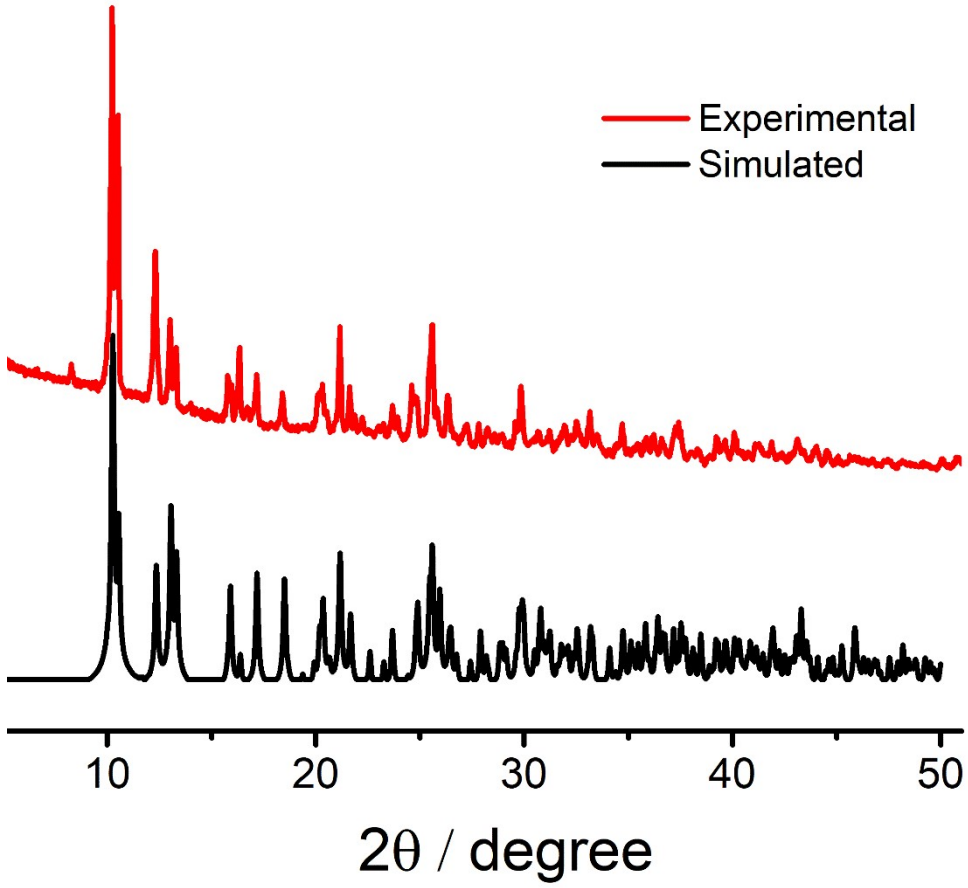

Fig. S6 Powder X-ray diffraction pattern of a bulk sample of **1**

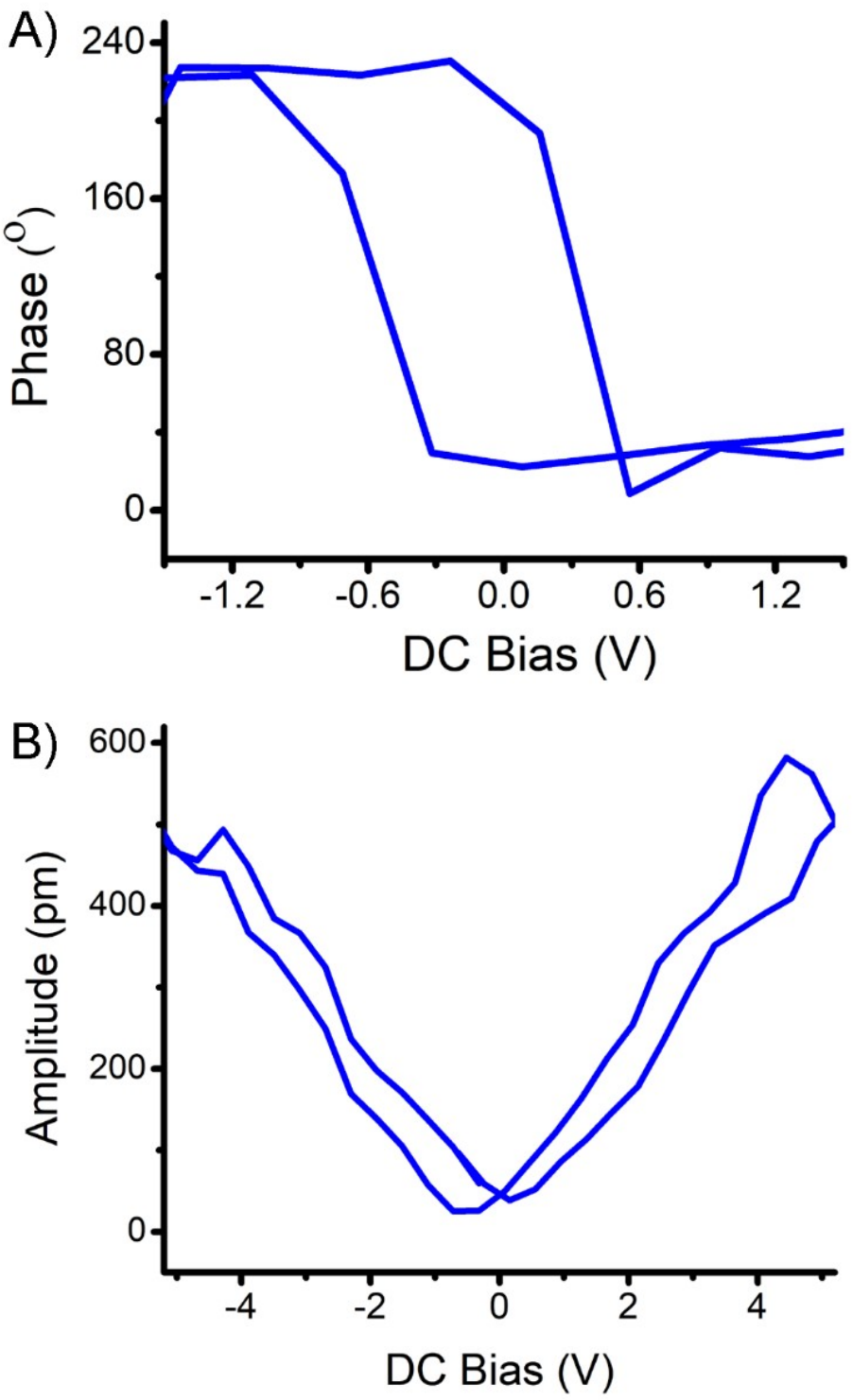

Fig. S7 (A) Phase-Voltage hysteresis loop and (B) Amplitude-Voltage butterfly loop observed through PFM analysis of thin film of **1** with tip voltage of 2 V.

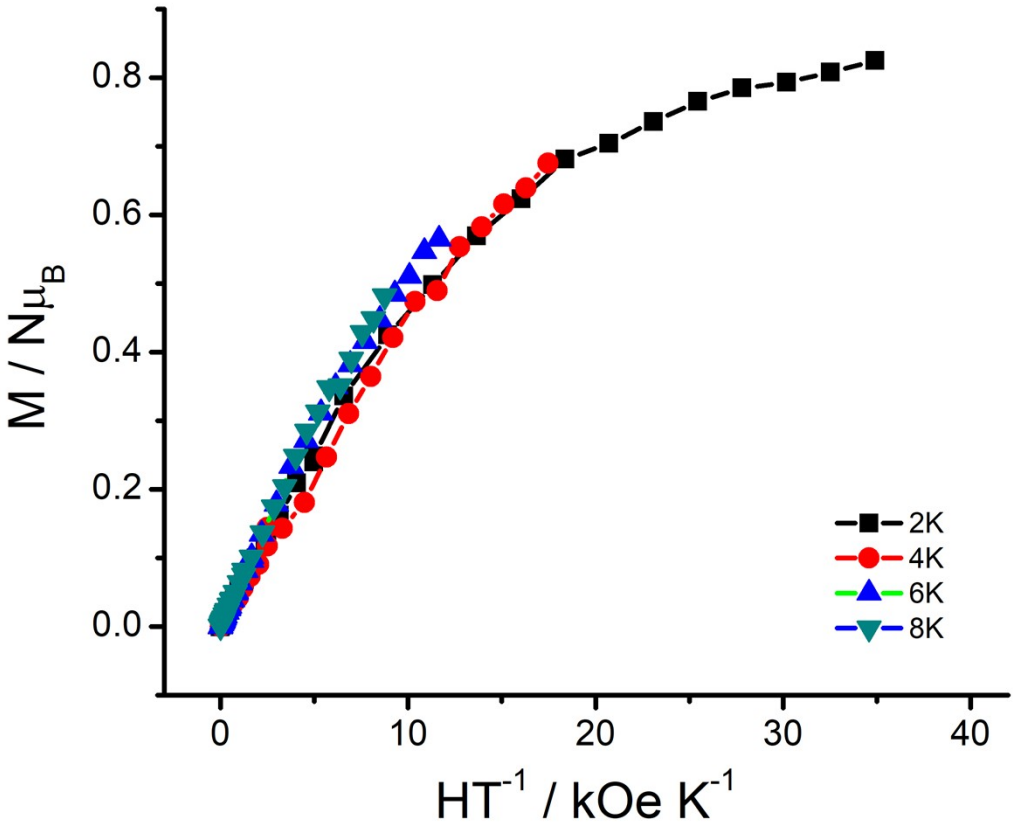

Fig. S8 Reduced magnetization curve for complex **1**

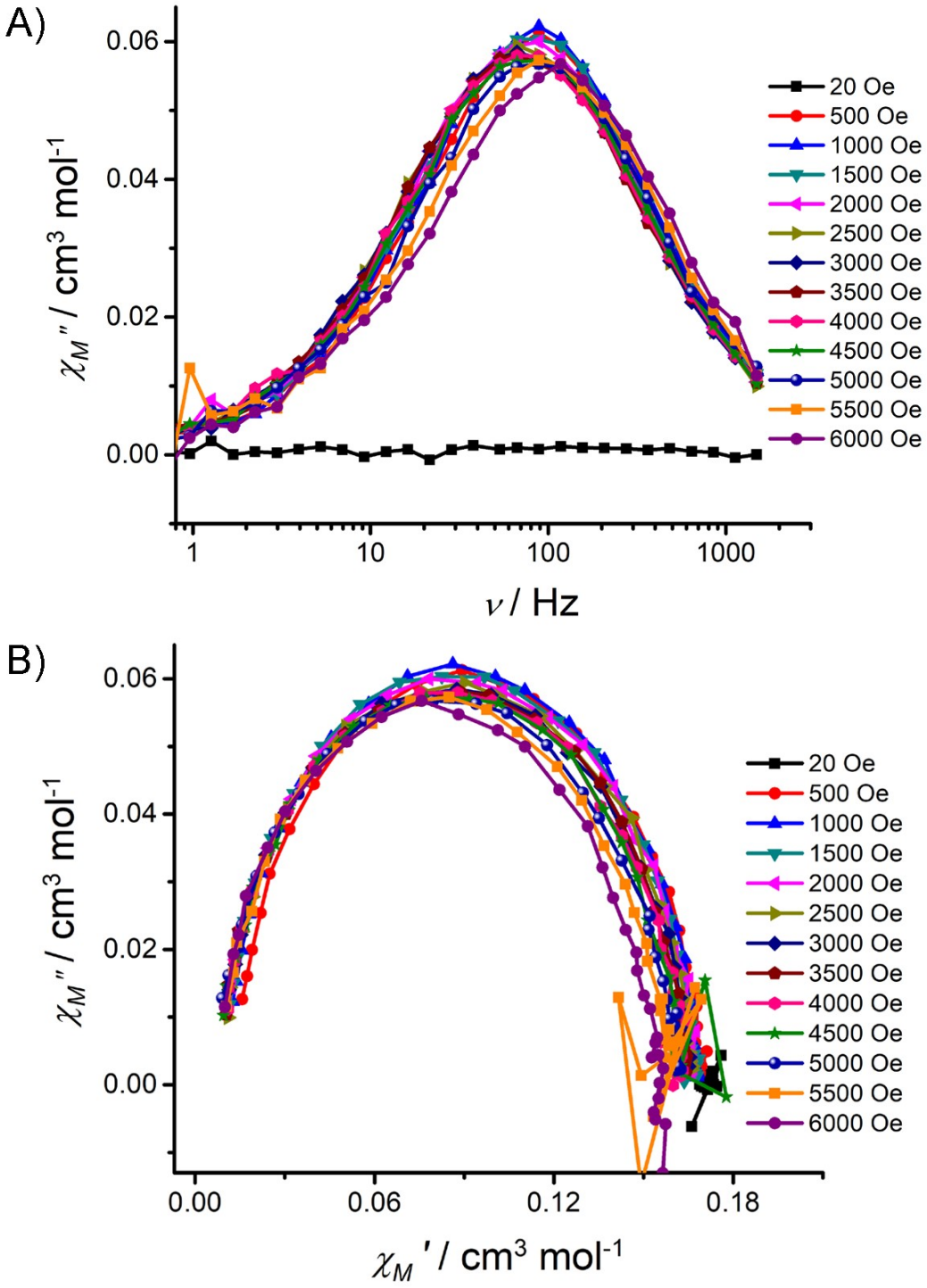

Fig. S9 (A) Frequency dependence of out-of-phase susceptibility and (B) Cole-Cole plot for polycrystalline sample of **1** recorded at 1.8 K temperature.

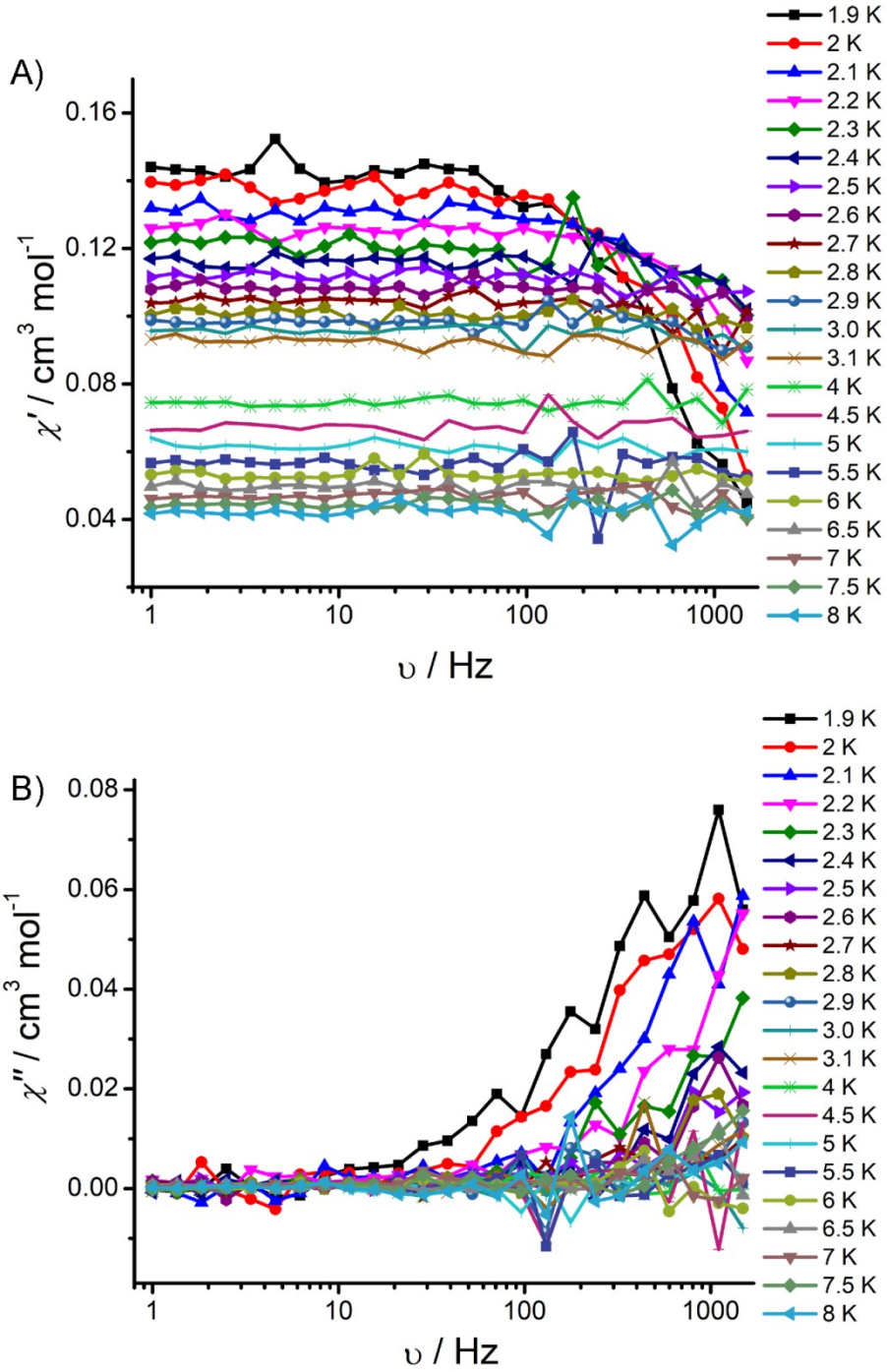

Fig. S10 (A) and (B) frequency dependence of in-phase and out-of-phase susceptibility respectively observed for polycrystalline sample of **1** in presence of dc magnetic field (H_{dc} = 1500 Oe)

$$\frac{1}{\tau} = \frac{1}{\tau_{QTM}} + \tau_0^{-1}\exp\left(\frac{-U_{eff}}{k_B T}\right) \quad \text{.....Equation S1}$$

References

1 A. S. Gajarushi, M. Wasim, R. Nabi, S. Kancharlapalli, V. R. Rao, G. Rajaraman, C. Subramaniam and M. Shanmugam, *Mater. Horiz.*, 2019, **6**, 743-750.

2 P. R. Spackman, M. J. Turner, J. J. McKinnon, S. K. Wolff, D. J. Grimwood, D. Jayatilaka and M. A. Spackman, *J. Appl. Crystallogr.*, 2021, **54**, 1006-1011.